Journal of Soil Science and Plant Nutrition

Combined effect of soil particle size fractions and engineered nanoparticles on phosphate sorption processes in volcanic soils evaluated by Elovich and Langmuir-Freundlich models

--Manuscript Draft--

Manuscript Number:	JSSP-D-21-01242R2
Full Title:	Combined effect of soil particle size fractions and engineered nanoparticles on phosphate sorption processes in volcanic soils evaluated by Elovich and Langmuir-Freundlich models
Article Type:	Original Paper
Funding Information:	Fondo Nacional de Desarrollo Científico y Tecnológico (FONDECYT) (1181050) — Dra. María de la Luz Mora Fondo Nacional de Desarrollo Científico y Tecnológico (FONDECYT) (1191018) — Dr. Nicolás Arancibia-Miranda Agencia Nacional de Investigación y Desarrollo (ANID) (21171685) — Dr. Jonathan Marcelo Suazo-Hernández
Abstract:	Abstract Purpose Engineered nanoparticles (ENPs) released into the environment can affect phosphate (Pi) availability in soils. In this study, we evaluated the effect of silver (Ag) or copper (Cu) ENPs (3 and 5%, w/w) on Pi sorption processes in soil particle size fractions. Methods The 2000-32 μm, 32-2 μm and <2 μm fractions were obtained from an agricultural volcanic soil by wet-sieving and sedimentation methods. The Elovich kinetic and Langmuir-Freundlich (L-F) isotherm models were used to describe the adsorption data obtained from batch experiments. Results The initial adsorption rate (α) was determined from the Elovich model to be 105% higher for the 2000-32 μm fraction and 203% higher for the 32-2 μm fraction than for the <2 μm fraction (671 mmol kg −1 min −1). Meanwhile, with both doses of Cu ENPs, the α values are increased for the soil size fractions, resulting in the formation of adsorption sites for Pi. However, with Ag ENPs, the α values are both increased and decreased for the different soil fractions; therefore, they can block or generate adsorption sites. The maximum adsorption capacity (q max) was determined from the L-F model to be 17% higher for the 32-2 μm fraction and 47% higher for the <2 μm fraction compared to that for the 2000-32 μm fraction (180 mmol kg −1). With both ENPs, the q max values are found to be between 1.1 and 1.9 times higher with respect to the 2000-32 μm fraction without ENPs. In the absence of ENPs the highest Pi desorption was found in the 32-2 μm fraction followed by 2000-32 μm fraction, and finally <2 μm fraction. Moreover, the Pi desorption decreased for soil size fractions with increasing Ag or Cu ENPs content, which was found to be more pronounced in the 32-2 μm fraction in the presence of Cu ENPs. Conclusions The presence of Ag and Cu ENPs increases Pi retention in soil size fractions, which can decrease soil fertility. Thus, future studies are recommended to find out the critical amounts of ENPs, which may favor Pi retention without any negative effects on agricultural soils.
Corresponding Author:	María de la Luz Mora, Ph.D. Bioren-Universidad de La Frontera Temuco, Araucania CHILE
Corresponding Author Secondary Information:	
Corresponding Author's Institution:	Bioren-Universidad de La Frontera
Corresponding Author's Secondary	

Institution:	
First Author:	Jonathan Marcelo Suazo-Hernández, Ph.D.
First Author Secondary Information:	
Order of Authors:	Jonathan Marcelo Suazo-Hernández, Ph.D.
	Erwin klumpp, Ph.D.
	Nicolás Arancibia-Miranda, Ph.D.
	Alejandra Jara, Ph.D.
	Patricia Poblete-Grant, Ph.D.
	Pamela Sepúlveda, Ph.D.
	Roland Bol, Ph.D.
	María de la Luz Mora, Ph.D.
Order of Authors Secondary Information:	
Author Comments:	
Response to Reviewers:	Response to Reviewers' Comments (Original manuscript no.: JSSP-D-21-01242_R2) We are thankful to the reviewers for their constructive comments and suggestions to improve the manuscript entitled "Combined effect of soil particle size fractions and engineered nanoparticles on phosphate sorption processes in volcanic soils evaluated by Elovich and Langmuir-Freundlich models" (submission no. JSSP-D-21-01242_R2). As indicated through track changes and highlighted texts in the revised manuscript, we have addressed all comments of the reviewers and listed our responses here as follows: Comments to the author (if any): Reviewer #4: This manuscript has been substantially improved after revision. The authors have taken my suggestions into full consideration. This revised work deserves to be published in JSSPN. R= We thank the reviewer for this positive evaluation of our manuscript. Anyway, I suggest to modify and improve the conclusions (l. 46-47 and l. 360-362). Because the massive deposition of ENP negatively affects soil fertility and plant growth (but non experiments are shown), probably is better to conclude that future studies are necessary to find the optimal amounts of ENPs (no massive deposition !) which may favor P retention without negative effect on soil fertility (see also comments of referee 3). R= We thank the reviewer for the suggestion. We have changed the abstract and conclusion. Lines 47-48: Lines 366-367. Reviewer #5: The authors have answered all comments from the reviewer and basically fulfilled the concerns raised. R= We thank the reviewer for the evaluation of our manuscript. However, I believe one problem is the authors should discuss the basic mechanism of P adsorption by the Ag and Cu nanoparticles and possibly the fate of the adsorbed P afterward. R= We thank the reviewer for the comment. In our previous paper (Suazo-Hernández et al. 2021), we reported that P was adsorbed through monodentate surface complexation on Cu ENPs, while it was adsorbed through hydrogen bonding on Ag ENPs (Niaura et al. 1997; White and Hjortkjaer 2014). Moreover, we concluded that due to the presence of ENPs in soil, solution pH decreased, and as a consequence, the electrostatic repulsion between P and the soil surface decreased, and thus the protonation of the surface hydroxyl groups of Fe/Al (hydr)oxides was promoted, which increased Pi adsorption through a ligand exchange mechanism. In addition, with Cu ENPs, the desorption of P from Volcanic soils was smaller than with Ag ENPs. These results can be explained by a chemisorption-like interaction between P and Cu ENPs

	(Suazo-Hernández et al. 2021). We have added this general idea to this manuscript in lines 335-340 and 346-347. References Niaura G, Gaigalas AK, Vilker VL (1997) Surface-enhanced Raman spectroscopy of phosphate anions: Adsorption on silver, gold, and copper electrodes. J Phys Chem B 101:9250–9262. https://doi.org/10.1021/jp970097k Suazo-Hernández J, Klumpp E, Arancibia-Miranda N, Poblete-Grant P, Jara A, Bol R, Mora MDLL (2021) Describing Phosphorus Sorption Processes on Volcanic Soil in the Presence of Copper or Silver Engineered Nanoparticles. Minerals 11:1–18. https://doi.org/10.3390/min11040373 White P, Hjortkjaer J (2014) Preparation and characterisation of a stable silver colloid for SER(R)S spectroscopy. J Raman Spectrosc 45:32–40. https://doi.org/10.1002/jrs.4412 Line 41~42 "…..in the order of 32-2 μm > 2000-32 μm > <2 μm….." seems not correct, please pay attention. R= We thank the reviewer for the comment. We have improved that sentence according our data. Lines 41-42.

Combined effect of soil particle size fractions and engineered nanoparticles on phosphate sorption processes in volcanic soils evaluated by Elovich and Langmuir-Freundlich models

Jonathan Suazo-Hernández[1,2,3], Erwin Klumpp[4], Nicolás Arancibia-Miranda[5,6], Alejandra Jara[2,3], Patricia Poblete-Grant[2], Pamela Sepúlveda[5,6,7], Roland Bol[4,8], María de la Luz Mora[2,3*]

[1]Doctoral Program in Science of Natural Resources, Universidad de La Frontera, Av. Francisco Salazar 01145, P.O. Box 54-D, Temuco, Chile

[2]Center of Plant, Soil Interaction and Natural Resources Biotechnology, Scientific and Biotechnological Bioresource Nucleus (BIOREN-UFRO), Universidad de La Frontera, Avenida Francisco Salazar 01145, Temuco, Chile

[3]Department of Chemical Sciences and Natural Resources, Universidad de La Frontera, Av. Francisco Salazar 01145, P.O. Box 54-D, Temuco, Chile

[4]Institute of Bio- and Geosciences, Agrosphere (IBG-3), Research Centre Jülich, 52425 Jülich, Germany

[5]University of Santiago of Chile (USACH), Faculty of Chemistry and Biology, Av. B. O'Higgins, 3363, Santiago, Chile

[6]University of Santiago of Chile (USACH), Center for the Development of Nanoscience and Nanotechnology (CEDENNA), 9170124, Santiago, Chile

[7]University of Santiago of Chile (USACH), Faculty of Science, Physics Department, Chile

[8]School of Natural Sciences, Environment Centre Wales, Bangor University, Bangor, UK

*Corresponding author: Dra. María de la Luz Mora; Universidad de La Frontera. UFRO

e-mail: mariluz.mora@ufrontera.cl

Abstract

Purpose

Engineered nanoparticles (ENPs) released into the environment can affect phosphate (Pi) availability in soils. In this study, we evaluated the effect of silver (Ag) or copper (Cu) ENPs (3 and 5%, w/w) on Pi sorption processes in soil particle size fractions.

Methods

The 2000-32 μm, 32-2 μm and <2 μm fractions were obtained from an agricultural volcanic soil by wet-sieving and sedimentation methods. The Elovich kinetic and Langmuir-Freundlich (L-F) isotherm models were used to describe the adsorption data obtained from batch experiments.

Results

The initial adsorption rate (α) was determined from the Elovich model to be 105% higher for the 2000-32 μm fraction and 203% higher for the 32-2 μm fraction than for the <2 μm fraction (671 mmol kg^{-1} min^{-1}). Meanwhile, with both doses of Cu ENPs, the α values are increased for the soil size fractions, resulting in the formation of adsorption sites for Pi. However, with Ag ENPs, the α values are both increased and decreased for the different soil fractions; therefore, they can block or generate adsorption sites. The maximum adsorption capacity (q_{max}) was determined from the L-F model to be 17% higher for the 32-2 μm fraction and 47% higher for the <2 μm fraction compared to that for the 2000-32 μm fraction (180 mmol kg^{-1}). With both ENPs, the q_{max} values are found to be between 1.1 and 1.9 times higher with respect to the 2000-32 μm fraction without ENPs. In the absence of ENPs the highest Pi desorption was found in the 32-2 μm fraction followed by 2000-32 μm fraction, and finally <2 μm fraction. Moreover, the Pi desorption decreased for soil size fractions with increasing Ag or Cu ENPs content, which was found to be more pronounced in the 32-2 μm fraction in the presence of Cu ENPs.

Conclusions

The presence of Ag and Cu ENPs increases Pi retention in soil size fractions, which can decrease soil fertility. Thus, future studies are recommended to find out the critical amounts of ENPs, which may favor Pi retention without any negative effects on agricultural soils.

Keywords: Engineered nanoparticles, Phosphate, Soil particle size fractions, Adsorption, Volcanic soil

1 Introduction

Engineered nanoparticles (ENPs) are defined as any intentionally produced particles that have a size that fluctuates in the range of 1-100 nm, which enables them to have a high surface/volume ratio, a large surface area, and a large number of reactive atoms on their surface (Auffan et al. 2009). ENPs possess unique, novel and enhanced electronic, chemical, and mechanical properties compared to larger-size particles with the same chemical composition (Auffan et al. 2009; He et al. 2019). These properties, together with the high industrial capacity to design and produce ENPs, have allowed their incorporation into products used in fields such as medical care, food, decontamination, transportation, industrial energy, and agriculture, among others (Ebrahimbabaie et al. 2020).

In agriculture, the use of nanoagrochemicals based on metallic silver (Ag), copper (Cu), iron (Fe), and aluminum (Al) ENPs is an alternative to traditional agrochemicals to treat infections in plants, reduce the amount of fertilizer added, and increase the growth, development, yield, and quality of plants without damaging productivity (Cota-Ruiz et al. 2020). In this sense, it is estimated that the concentration of metallic and metal oxide ENPs deposited in agricultural soils will increase from 3 ng kg^{-1} in 2017 to 30 g kg^{-1} for 2050 (Giese et al. 2018). Among the most commonly used metallic ENPs to treat and control diseases, Ag and Cu stand out due to their antibacterial, virucidal, and antifungal properties (Arya et al. 2018). In this sense, both ENPs demonstrate the ability to inhibit the growth of pathogenic fungi (Hashmi et al. 2019; Malandrakis et al. 2021) and Gram-

negative and Gram-positive bacteria (Benassai et al. 2021; Rolim et al. 2019). Additionally, because Cu is a micronutrient for plants, Cu ENPs can promote the growth of tomato plants (Lopez-Lima et al. 2021), increase the total seed number and grain yield in maize (Van Nguyen et al. 2021) and improve the physiology of alfalfa (Cota-Ruiz et al. 2020). A potential consequence of the massive application of Ag and Cu ENPs in agricultural practices is their uncontrolled release into the natural environment and particularly into agroecosystems, making it necessary to study the behavior and implications of ENPs in soils. To date, there have been several studies on the transformations, fate, toxicity, and transport of ENPs in the soil matrix (Abbas et al. 2020; He et al. 2019; Parada et al. 2019). Nevertheless, few investigations have evaluated the effects of ENPs on processes and reactions of elements in soils, such as complexation, dissolution, precipitation, coprecipitation, and sorption (adsorption/desorption). In particular, adsorption/desorption processes play an essential role in regulating element availability (Yang et al. 2019). In soils, phosphorus (P) is among the most essential elements for plant growth and is taken up by plants mainly in the form of inorganic phosphate ($H_2PO_4^-$) (Parra-Almuna et al. 2020). In this context, phosphate (Pi) sorption studies in the presence of ENPs have been focused on whole soil (<2 mm), which have demonstrated that iron oxide ENPs (Koopmans et al. 2020), Al_2O_3 and TiO_2 ENPs (Taghipour and Jalali 2015) and Cu or Ag ENPs (Suazo- Hernández et al. 2021) can increase the soil capacity to retain Pi. In our recent study (Suazo-Hernández et al. 2021), we found that with increased dosage of Cu or Ag ENPs from 0 to 5% (w/w), Pi adsorption is increased between 1.3 and 2.0 times for an Andisol with total organic matter (OM) and with partial removal of OM in relation to systems without ENPs. Consequently, a higher Pi accumulation can decrease the stoichiometric C:N:P molar ratio, affecting nutrient levels and the optimal growth and development of plants (Song et al. 2014).

Soil is composed of various particle size fractions (Sparks 2003), which are relevant in the different physical, chemical, and biological processes that occur in the soil matrix. In relation to this, the adsorption/desorption processes of Pi on soil fractions not only differ greatly from the whole soil, but they also vary markedly between the individual particle size fractions (Acosta et al. 2011). In general, sorption studies have shown that Pi adsorption capacity increases with decreasing particle size (Atalay 2001; Cui et al. 2019). In volcanic soils, Pi adsorption on the clay size fraction is higher and stronger than that on the whole soil, which is associated with the greater presence of amorphous and poorly crystallized minerals Fe/Al oxides and allophane (Borie et al. 2019; Escudey and Galindo 1983; Redel et al. 2016). Amorphous allophane aluminosilicate is the main component of the clay fraction, representing > 50% of the mass, while in whole volcanic soils, it is close to 5% (Molina et al. 2007; Mora and Barrow 1996).

To evaluate the implication of ENPs on the whole volcanic soil capacity to accumulate or release Pi, it is essential to explore Pi sorption processes on different soil fractions in the presence of ENPs. The aim of our study was to evaluate the combined effect of soil particle size fractions and ENPs on Pi sorption processes in a volcanic soil by using Elovich kinetic and Langmuir-Freundlich isotherm models.

2 Materials and methods

2.1 Chemicals and Cu and Ag ENPs used

$AgNO_3$, $CuCl_2 \cdot 2H_2O$, L-ascorbic acid, KH_2PO_4, KCl, KOH, HCl analytical grade (Merck), and double distilled water were used. The Cu and Ag ENPs stabilized with L-ascorbic acid used were synthesized and characterized in our previous study (Suazo-Hernández et al. 2021). Briefly, Cu ENPs (or Ag ENPs) were synthesized by mixing 10.0 mmol L^{-1} $CuCl_2 \cdot 2H_2O$ (or 10.0 mmol L^{-1} $AgNO_3$) in 50 mL double distilled water. An Erlenmeyer flask containing the solution was heated in a water bath at 80 °C with magnetic stirring, and 50 mL of 1.0 mol L^{-1} L-ascorbic acid solution

was added dropwise into the flask while stirring. The aqueous dispersion of Cu and Ag ENPs had a diameter ranging between 7 nm and 29 nm (Suazo-Hernández et al. 2021). The isoelectric point of Cu ENPs was 2.7, whereas Ag ENPs had a negatively charged surface in the pH range from 2.5 to 8.5.

2.2 Soil used and its fractionation

The soil used was an Andisol belonging to the Santa Barbara series in southern Chile (36° 50´ S; 113 71° 55´ W). The soil sample was taken from the top 20 cm of the soil horizon, and it was passed through a 2 mm mesh sieve and dried in air (1 day at room temperature). The whole soil was fractionated into three particle size fractions according to a wet-sieving method assisted by ultrasonication and sedimentation following the methodology proposed by Genrich and Bremner (1974) and modified by our laboratory group (Calabi Floody et al. 2011; Escudey et al. 2001) to separate soil fractions from Andisols. Briefly, 100 g of original soil was weighed and added to 360 mL of double distilled water into glass bottles. The soil suspension was left to shake at 200 rpm overnight to be passed through a 32 μm sieve (soil particle sizes ranging from 2000 μm to 32 μm represented the sand/coarse silt mixture fraction), and it was washed repeatedly with double distilled water. Subsequently, 200 mL of <32 μm-double distilled water suspension was ultrasonically dispersed by applying 7,500 J g^{-1} (repeatedly) using a Vibra Cell High-Intensity model VC 750 (Sonics and Materials Inc. Danbury, CT) equipment. The <32 μm fraction suspension was placed in a one-liter graduated cylinder, from which the size fraction <2 μm (clay size fraction) was obtained by sedimentation under gravity, following Stokes law, from the first 20 cm, and the remaining suspension corresponded to the size fraction ranging from 32 μm to 2 μm (represented as the fine silt fraction). The separated <2 μm suspension was sedimented by adding 1.8 mol L^{-1} NaCl and washed four times with double distilled water to minimize the excess of NaCl. Finally, the soil fractions were freeze-dried and stored for further analysis.

2.3 Physicochemical characterization of the soil particle size fractions

The pH of the soil fractions was determined in a 1:2.5 soil-water suspension using the method described by Sadzawka et al. (2006) for Chilean Andisols. The total nitrogen (N) and carbon (C) contents were determined by the dry combustion method using a EuroEA 3000 Series elemental analyzer (Euro Vector Inc, Milan, Italy). Total phosphorus was extracted by sodium hypobromite (NaBrO) (Dick and Tabatabai 1976) and analyzed according to Murphy and Riley (1962). The stoichiometric C:N, C:P, N:P, and C:N:P molar ratios are shown. Exchangeable aluminum (Al) was extracted with KCl (1 mol L^{-1}) (Sadzawka et al. 2006) and analyzed using a Unicam model Solaar 969 atomic absorption spectrophotometer (AAS) (Unicam Ltd, Cambridge, England). Exchangeable cations (Mg, Ca, K and Na) were extracted with NH_4Ac (1 mol L^{-1}, pH 7.0) and analyzed by AAS (Sadzawka et al. 2006). The effective cation exchange capacity (ECEC) was determined as the sum of exchangeable Al plus the exchangeable cations. The specific surface area in the soil fractions was calculated by the Brunauer–Emmett–Teller (BET) method for N_2 adsorption with a Quantachrome Nova 1000e (Quantachrome Instruments, Boynton Beach, FL, USA). The zeta potential (ZP) of each soil fraction was measured with a Nano ZS apparatus (Malvern Instruments, Worcestershire, UK). Additionally, the ZP of the soil fractions was determined post-adsorption for Pi in the presence and absence of 5% Ag or Cu ENPs using high point adsorption isotherms.

2.4 Batch adsorption assays

Batch techniques were performed to determine the amount of Pi adsorbed onto the particle size fractions of soil with and without Ag or Cu ENPs. In 50 mL polypropylene centrifuge tubes, 0, 3, and 5% Ag or Cu ENPs were added to 0.5 g of each soil fraction (w/w).

The kinetic study was carried out with 20 mL taken from an initial stock solution of 6.47 mmol L^{-1} of Pi and a pH of 5.5 ± 0.2. The amount of Pi present in the solution was determined in time

intervals ranging between 2.5 and 1440 min. Adsorption isotherms on soil particle size fractions were determined using 20 mL of Pi solution at different concentrations (0.02 − 9.71 mmol L^{-1}) at pH 5.5 ± 0.2. The soil suspensions used for adsorption isotherm experiments were stirred for 1440 min. Kinetic and equilibrium adsorption analyses were conducted using KCl 0.01 mol L^{-1} as ionic strength, and the suspensions were stirred at 200 rpm at 20 ± 2 °C. The soil fraction samples were centrifuged for 10 min at 10,000 rpm using a Sorvall Model RC-5B Plus centrifuge. After shaking the soil fraction samples, the supernatant was filtered through syringe filters with a 0.45 μm pore size. The Pi amount in the supernatant solution was determined using a Rayleigh UV-2601 spectrophotometer (BRAIC, Beijing, China) at a wavelength of 880 nm by the molybdate-blue colorimetric procedure (Murphy and Riley 1962). The concentration of Pi adsorbed at time t (q_t, mmol kg^{-1}) on soil fractions with and without Ag or Cu ENPs was determined by the following equation:

$$q_{t=}\frac{(C_0 - C_t)V}{(w)} \quad (1)$$

where Co (mmol L^{-1}) is the initial concentration of Pi, C_t (mmol L^{-1}) is the concentration of Pi at time t or the equilibrium concentration, w is the mass (kg) of the soil fractions used and V is the volume (L) of the adsorptive solution.

2.5 Modeling of the adsorption assays

The kinetic data for Pi adsorption on different soil fractions were fitted by the Elovich model. This model describes an adsorption process on a heterogeneous solid substrate (Cea et al. 2010). The Elovich model is represented by equation 2:

$$q_t = \frac{1}{\beta}\ln(\alpha\beta t) \quad (2)$$

where q_t (mmol kg^{-1}) is the concentration of Pi adsorbed at time t (min), α (mmol kg^{-1} min^{-1}) is associated with the initial adsorption rate and β (mmol kg^{-1}) is associated with the number of sites available for Pi adsorption and the desorption constant.

Using the parameters of the Elovich model, it is possible to obtain the equilibrium constant (K_{eq}) for the Pi adsorption process through equation 3 (Cea et al. 2010):

$$K_{eq} = \frac{\alpha}{\beta} \quad (3)$$

The adsorption data obtained from Pi isotherms for different soil particle size samples were described by the Langmuir-Freundlich (L-F) model. The L-F model describes chemical adsorption on an energetically heterogeneous surface (Yin et al. 2018). The L-F model is represented by the following expression:

$$q_e = \frac{q_{max} K_{L-F} C_e^{\frac{1}{n}}}{1 + K_{L-F} C_e^{\frac{1}{n}}} \quad (4)$$

where q_e (mmol kg^{-1}) is the concentration of Pi adsorbed at equilibrium, q_{max} (mmol kg^{-1}) is the maximum adsorption capacity, K_{L-F} (L kg^{-1}) is the L-F affinity parameter, C_e (mmol L^{-1}) is the concentration of Pi in solution at equilibrium and 1/n is the heterogeneity factor.

2.6 Batch desorption assays

Desorption experiments for Pi were performed to analyze the effect of ENPs on the potential Pi release from soil fractions. Once the Pi adsorption isotherm procedure ended, the supernatant from the highest points was replaced three times (repeatedly) with 20 mL of double-distilled water. Then, the suspensions were stirred at 200 rpm in an orbital shaker at 20 ± 2 °C for 24 h, and the Pi in the solution was analyzed similar to that in the adsorption experiments. Desorption (%) was calculated from the amount of Pi adsorbed in the soil fractions and the Pi desorbed into aqueous solution by using equation 5:

$$\text{Desorption (\%)} = \frac{\text{Amount of Pi desorbed}}{\text{Amount of Pi adsorbed}} \text{ x } 100 \quad (5)$$

2.7 Data analysis

All results were recorded as the mean of three replicates, and all calculations were based on the average ± standard deviation. Statistical analyses were carried out using the software program Origin Pro 9.0.

3 Results

3.1 Characterization of particle size fractions in a volcanic soil

The 32-2 μm fraction was the dominant fraction with a content of 59.3%, followed by the <2 μm size fraction with a content of 24.5% and finally by the 2000-32 μm fraction with a content of 16.2% of the mass of the original soil (Table 1). The pH values obtained for the 2000-32 μm, 32-2 μm, and <2 μm size fractions were 5.6, 6.0, and 6.2, respectively. The total amount of P, C, and N in units of g kg^{-1} and specific surface area followed the order of <2 μm > 32-2 μm > 2000-32 μm, and for ECEC, the order was <2 μm > 2000-32 μm > 32-2 μm (Table 1). On the other hand, the stoichiometric C:N, C:P, and C:N:P molar ratios followed the soil fraction order of 2000-32 μm > 32-2 μm > <2 μm. Finally, the zeta potential (ZP) of the soil size fractions was observed to be negative in all pH ranges studied (Fig. 1).

3.2 Pi adsorption kinetics

As shown in Figure S1a–f, the prolongation of the agitation time and increase in Ag or Cu ENPs content provokes an increase in the total amount of Pi adsorbed on different soil fractions. In most cases, the kinetic adsorption of Pi on the soil fraction is separated into a fast stage (≤ 45 min) and a slow stage (> 45 min) (Figs. S1a–f and 2Sa–f). Specifically, during the first 45 min, approximately 39%, 42%, and 46% of the total amount of Pi added (248.9 mmol kg^{-1}) is removed by 32-2 μm, 2000-32 μm, and <2 μm size fractions, respectively. Meanwhile, with Ag or Cu ENPs,

231 at least 50% of the total amount of Pi added is removed by the soil size fractions within 45 min.
232 For most kinetic systems, the adsorbed amount increases slightly until reaching equilibrium at >720
233 min (Fig. S1a–f).
234 The correlation coefficient values (r^2) for the fits obtained using the Elovich model of Pi adsorption
235 by soil particle size fractions with and without Ag or Cu ENPs (Fig. 2a–f) range between 0.956
236 and 0.992, and the chi-squared (χ^2) value ranges from 5 to 182 (Table 2). Without ENPs, the initial
237 adsorption rate (α) from the Elovich model is 105% higher for the 2000-32 μm fraction and 203%
238 higher for the 32-2 μm fraction than for the <2 μm fraction (671 mmol kg^{-1} min^{-1}). In the presence
239 of ENPs, the α values show an increase of between 47.0% and 1460% with respect to the systems
240 without ENPs, except for the 3% Ag ENPs/32-2 μm and 5% Ag ENPs/32-2 μm and 2000-32 μm
241 fraction systems. The sequence followed by the number of sites available for the adsorption and
242 desorption constant (β) was 2000-32 μm > 32-2 μm > <2 μm, and with ENPs, the β values decrease
243 in relation to systems without ENPs. In the presence of both ENPs, the log K_{eq} values are higher
244 than those without ENPs, except for the 3 and 5% Ag ENPs-32-2 μm systems (Table 2).

245 **3.3 Pi adsorption isotherms**

246 Figure 3a–f show that Pi adsorption decreases with increasing soil particle size fractions, indicating
247 that the adsorption capacity of Pi by fine soil particles is greater than that for coarse particles. In
248 addition, when increasing the ENP dosage, Pi adsorption increases, and the tendency is similar to
249 that found for systems without ENPs.
250 The adsorption isotherms obtained for Pi on soil fractions with and without ENPs are well fitted
251 by the Langmuir-Freundlich (L-F) model (Table 3, $r^2 \geq 0.943$ and $\chi^2 \leq 419$). The Pi maximum
252 adsorption capacity (q_{max}) for the 32-2 μm and <2 μm fractions is approximately 17% and 47%,
253 respectively, higher than that for the 2000-32 μm soil fraction (180.01 mmol kg^{-1}). Meanwhile,
254 with 5% ENPs, the q_{max} values increase in a range between 36% and 54% for the 32-2 μm fraction

and between 89% and 91% for the <2 μm fraction in relation to the 2000-32 μm fraction without ENPs. The sequence followed by the affinity parameter (K_{L-F}) value is <2 μm > 2000-32 μm > 32-2 μm (Table 3). With Ag or Cu ENPs, the K_{L-F} values increase between 1.3 and 10.0 times with respect to the systems without ENPs and are higher with Cu ENPs. The constant related to the degree of heterogeneity (n) shows the sequence of <2 μm > 2000-32 μm > 32-2 μm. With increasing Ag or Cu ENPs content, the n values decrease between 0.4 and 0.7 times in relation to the systems without ENPs and are lower with Cu ENPs.

3.4 Pi desorption in water

Desorption investigations enable us to predict the availability and potential mobility of Pi adsorbed on soil particle size fractions. The results reveal that after treatment with double distilled water (three times), the Pi desorption (%) is decreased as follows: 32-2 μm > 2000-32 μm > <2 μm (Table 4). Meanwhile, with Ag or Cu ENPs, the amount of Pi desorbed from different soil fractions is decreased between 0.33 and 0.85 times in comparison with the systems without ENPs, and it is lower with Cu ENPs. In all systems with ENPs, the 32-2 μm soil fraction shows the lowest Pi desorption (%) (Table 4).

4 Discussion

The <2 μm fraction shows higher amounts of total C, N, and P (g kg^{-1}) and values of ECEC ($cmol_{(+)}$ kg^{-1}) than the 32-2 μm and 2000-32 μm fractions. These results can be attributed to colloid particles (1-1000 nm) and allophane contained in the <2 μm size fraction (Liu et al. 2019), which have high reactivity and specific surface area, and thus, may contain more binding sites to strongly accumulate/adsorb OM, nutrients and cations. Several researchers have reported similar results for the smallest particle size fractions extracted from Aridisol (Fernández et al. 2015) and Mollisol soils (Chaparro et al. 2020).

According to Spohn (2020), the values of the stoichiometric C:N, C:P, and C:N:P molar ratios obtained indicate that in the <2 μm fraction, there is a low mineralization of organic P compounds compared to other soil fractions. In contrast, the values for the stoichiometric relationships obtained for the 2000-32 μm and 32-2 μm fractions show that C, N, and P are available to be taken up by microorganisms and plants. Similar results were reported by Jiménez et al. (2008) for the stoichiometric relationship for different particle size fractions extracted from an Inceptisol soil in northeastern Costa Rica. On the other hand, the highest negative surface charge shown by the <2 μm size fraction was due to the high amount of organic carbon (OC) contained (Table 1) (Calabi-Floody et al. 2011; Escudey et al. 2001).

The Pi adsorption kinetics with and without ENPs indicate two separate steps, whereby adsorption is not only limited to the external surface area of the soil particles but intraparticle diffusion can also occur (Linquist et al. 1997). In the same way, several studies, Barrow (2015; 2021) and Barrow et al. (2021), have reported that the kinetic adsorption mechanism for Pi on soils occurs via two steps.

All the adsorption isotherms were L-type, showing that the soil fractions with and without ENPs have a high affinity for Pi (Fig. 3a–f). In particular, for the 2000-32 μm and 32-2 μm fractions, the isotherms reaches a plateau but not for the <2 μm size fraction. This indicates that the <2 μm fraction still has available sites for Pi adsorption (Limousin et al. 2007). In the presence of Ag or Cu ENPs, the adsorption isotherms did not reach a plateau, suggesting that both ENPs contribute to the formation of new adsorption sites for Pi molecules in different soil fractions (Zhou et al. 2005). This observation may be supported by the zeta potential values obtained from Pi adsorption on soil fractions in the presence of both ENPs, which are less negative than systems without ENPs (Fig. 4a–c).

The Elovich kinetic and L-F isotherm models satisfactorily describe the Pi adsorption, which indicates that chemical interactions are involved in Pi adsorption on the highly heterogeneous surface of soil size fractions (Maslova et al. 2020). Nevertheless, with increasing Ag or Cu ENPs content, the n values decrease (Table 3), which implies that the presence of ENPs decreases the degree of surface heterogeneity (Chatterjee and Woo 2009). In other words, ENPs can coat the heterogeneous surface sites of the fractions and confer to them the characteristics of a rather energetically homogeneous surface.

Based on α values obtained from the Elovich model, Pi adsorbs the fastest on the adsorption sites of the 32-2 μm fraction. In the presence of Cu ENPs, the α values always increase; therefore, ENPs improve the accessibility of adsorption sites from soil fractions for Pi binding at the beginning of the adsorption process. This phenomenon can be associated with the small size and high reactivity of the Cu nanoparticles. Meanwhile, Ag ENPs lead to both an increase and decrease in the α values, which indicates that ENPs can (i) promote the adsorption sites by Pi, (ii) compete with Pi for available surface sites and/or (iii) block the soil pores, preventing fast Pi diffusion to adsorption sites. Thus, Ag and Cu ENPs show different behavior for the α values, contrary to our previous study (Suazo-Hernández et al. 2021). This difference suggests that the behavior of ENPs might be regulated by the physicochemical properties of the soil fractions as well as the dosage and type of ENPs. In all cases, the α values are higher than β, which shows greater viability of Pi adsorption than the desorption process (Soliemanzadeh et al. 2016).

According to the L-F model, the <2 μm fraction shows the highest q_{max} value for the adsorption of Pi (Table 3). This can be explained by its larger specific surface area, ECEC, especially Ca^{2+} and Mg^{2+} (Table 1), and possibly due to the higher presence of poorly crystallized and amorphous Al/Fe oxides and allophane compared to the 2000-32 μm and 32-2 μm fractions (Borie et al. 2019; Escudey and Galindo 1983; Redel et al. 2016). Similar results have been reported for Entisol

(Atalay 2001) and Ultisol soils (Linquist et al. 1997). These properties are also contributed to soils with a high percentage of <2 μm particles having a great Pi adsorption capacity (Sun et al. 2020; Zhao et al. 2018). For instance, Zhao et al. (2018) reported that the soil clay content is one of the most relevant factors in the Pi adsorption capacity in Oxisol soils. When increasing the ENPs content from 0 to 5% in the 2000-32 μm, 32-2 μm, and <2 μm fractions, the q_{max} values are increased by approximately 24.2% by adding Ag ENPs and by 32.2% by adding Cu ENPs. It was shown in our previous work (Suazo-Hernández et al. 2021) using the Langmuir model that by increasing the ENP content from 0 to 5%, the q_{max} values of Pi for Andisol are increased by 46% and 54% following Cu ENPs and Ag ENPs addition, respectively. These effects were attributed to a decrease in soil solution pH from 5.4 to pH values between 5.0 and 3.8, which is due to the coating of ENPs with L-ascorbic acid and probably some dissolved L-ascorbic acid. As a consequence, the electrostatic repulsion between Pi and the soil surface is decreased, and the protonation of the surface hydroxyl groups of Fe/Al (hydr)oxides is promoted, increasing Pi adsorption through a ligand exchange mechanism (Suazo-Hernández et al. 2021). In addition, we reported that Pi could be adsorbed through hydrogen bonding on Ag ENPs, while on Cu ENPs it could be adsorbed through monodentate surface complexation (Suazo-Hernández et al. 2021).

The lowest percent Pi desorption and the highest K_{L-F} value shown for the <2 μm fraction indicate that the binding between <2 μm and Pi molecules is more favorable. In a similar manner, Linquist et al. (1997) found that Pi desorption in an Ultisol soil is inversely proportional to soil particle size fractions. Moreover, with the presence of Ag or Cu ENPs, the percent of Pi desorption is decreased, and the K_{L-F} and log K_{eq} values are increased in relation to the system without ENPs, indicating that Ag or Cu ENPs enhance the capacity in the solid phase of soil fractions to retain Pi. At the same time, the results indicate that with Cu ENPs, there is a stronger affinity of Pi to the surface of the soil fractions. A decrease in the availability of Pi in soils due to the presence of ENPs has been

reported previously (Suazo-Hernández et al. 2021; Koopmans et al. 2020). It was found that with increasing Ag or Cu ENPs dosage from 0 to 5%, Pi desorption from soil is decreased between 0.30 and 0.99 times with respect to systems without ENPs (Suazo-Hernández et al. 2021). On the other hand, the 32-2 μm fraction with ENPs shows the lowest desorption of Pi and the highest adsorption. Therefore, in that fraction, ENPs can lead to a higher increase in the retention of Pi.

5 Conclusions

In this article, we show an effect-oriented study of phosphate (Pi) adsorption on soil fractions with and without Ag or Cu ENPs by using Elovich kinetic and Langmuir-Freundlich (L-F) isotherm models. The results indicate that in the absence of ENPs, the initial adsorption rate (α) follows the order of <2 μm < 2000-32 μm < 32-2 μm. With Cu ENPs, the α values are increased for soil fractions, but with Ag ENPs, the α values are both increased and decreased for the soil fractions. The maximum Pi adsorption capacity (q_{max}) obtained from the L-F model follows the order of <2 μm > 32-2 μm > 2000-32 μm. In the presence of both ENPs, the q_{max} values for the soil fractions are found to be between 1.1 and 1.9 times higher with respect to the 2000-32 μm fraction without ENPs (180 mmol kg^{-1}). Both ENPs enhance Pi retention in the soil fractions, which is more pronounced in the 32-2 μm fraction with Cu ENPs. Thus, the deposition of ENPs in agricultural soils can favor the Pi retention process in various soil fractions, negatively affecting soil fertility. In the future, more research is necessary to determine the amounts of ENPs, which may favor Pi retention without any endangering of agricultural systems.

Acknowledgments Special thanks to Technological Bioresource Nucleus (BIOREN-UFRO) and Soil and Plant Laboratory. Patricia Poblete-Grant acknowledges ANID-FONDECYT/Post-Doctoral Grant N° 3210228. Jonathan Suazo-Hernández acknowledges Beca de Formación de Investigadores Postdoctorales UFRO 2022.

Funding This work was supported by FONDECYT Project Nº 1181050, 1191018 and ANID Ph.D. scholarships Nº 21171685.

Declarations

Competing interest The authors declare no conflict of interest

Ethics Approval Not applicable.

References

Abbas Q, Yousaf B, Amina, Ali MU, Munir MAM, El-Naggar A, Rinklebe J, Naushad M (2020) Transformation pathways and fate of engineered nanoparticles (ENPs) in distinct interactive environmental compartments: A review. Environ Int 138:105646. https://doi.org/10.1016/j.envint.2020.105646

Acosta JA, Martínez-Martínez S, Faz A, Arocena J (2011) Accumulations of major and trace elements in particle size fractions of soils on eight different parent materials. Geoderma 161:30–42. https://doi.org/10.1016/j.geoderma.2010.12.001

Arya A, Gupta K, Chundawat TS, Vaya D (2018) Biogenic Synthesis of Copper and Silver Nanoparticles Using Green Alga *Botryococcus braunii* and Its Antimicrobial Activity. Bioinorg Chem Appl 2018:1-9. https://doi.org/10.1155/2018/7879403

Atalay A (2001) Variation in Phosphorus Sorption with Soil Particle Size. Soil Sediment Contam An Int J 10:317–335. https://doi.org/10.1080/20015891109284

Auffan M, Rose J, Bottero J-Y, Lowry G V, Jolivet J-P, Wiesner MR (2009) Towards a definition of inorganic nanoparticles from an environmental, health and safety perspective. Nat Nanotechnol 4:634–41. https://doi.org/10.1038/nnano.2009.242

Barrow NJ (2021) Comparing two theories about the nature of soil phosphate. Eur J Soil Sci 72:679–685. https://doi.org/10.1111/ejss.13027

Barrow NJ (2015) A mechanistic model for describing the sorption and desorption of phosphate by soil. Eur J Soil Sci 66:9–18. https://doi.org/10.1111/ejss.12198_2

Barrow NJ, Debnath A, Sen A (2021) Effect of pH and prior treatment with phosphate on the rate and amount of reaction of soils with phosphate. Eur J Soil Sci 72:243–253. https://doi.org/10.1111/ejss.12968

Benassai E, Del Bubba M, Ancillotti C, Colzi I, Gonnelli C, Calisi N, Salvatici MC, Casalone E, Ristori S (2021) Green and cost-effective synthesis of copper nanoparticles by extracts of non-edible and waste plant materials from *Vaccinium* species: Characterization and antimicrobial activity. Mater Sci Eng C 119: 111453. https://doi.org/10.1016/j.msec.2020.111453

Borie F, Aguilera P, Castillo C, Valentine A, Seguel A, Barea JM, Cornejo P (2019) Revisiting the Nature of Phosphorus Pools in Chilean Volcanic Soils as a Basis for Arbuscular Mycorrhizal Management in Plant P Acquisition. J Soil Sci Plant Nutr 19:390–401. https://doi.org/10.1007/s42729-019-00041-y

Calabi-Floody M, Bendall JS, Jara AA, Welland ME, Theng BKG, Rumpel C, Mora ML (2011) Nanoclays from an Andisol: Extraction, properties and carbon stabilization. Geoderma 161:159–167. https://doi.org/10.1016/j.geoderma.2010.12.013

Cea M, Seaman JC, Jara A, Mora ML, Diez MC (2010) Kinetic and thermodynamic study of chlorophenol sorption in an allophanic soil. Chemosphere 78:86–91. https://doi.org/10.1016/j.chemosphere.2009.10.040

Chaparro MAE, Moralejo M del P, Böhnel HN, Acebal SG (2020) Iron oxide mineralogy in Mollisols, Aridisols and Entisols from southwestern Pampean region (Argentina) by environmental magnetism approach. Catena 190: 104534. https://doi.org/10.1016/j.catena.2020.104534

Chatterjee S, Woo SH (2009) The removal of nitrate from aqueous solutions by chitosan hydrogel beads. J Hazard Mater 164:1012–1018. https://doi.org/10.1016/j.jhazmat.2008.09.001

Cota-Ruiz K, Ye Y, Valdes C, Deng C, Wang Y, Hernández-Viezcas JA, Duarte-Gardea M, Gardea-Torresdey JL (2020) Copper nanowires as nanofertilizers for alfalfa plants: Understanding nano-bio systems interactions from microbial genomics, plant molecular responses and spectroscopic studies. Sci Total Environ 742:140572. https://doi.org/10.1016/j.scitotenv.2020.140572

Cui H, Ou Y, Wang L, Wu H, Yan B, Li Y (2019) Distribution and release of phosphorus fractions associated with soil aggregate structure in restored wetlands. Chemosphere 223:319–329. https://doi.org/10.1016/j.chemosphere.2019.02.046

Dick WA, Tabatabai MA (1977) An Alkaline Oxidation Method for Determination of Total Phosphorus in Soils. Am Soc Agron 41:501–514. https://doi.org/10.2136/sssaj1977.03615995004100030015x

Ebrahimbabaie P, Meeinkuirt W, Pichtel J (2020) Phytoremediation of engineered nanoparticles using aquatic plants: Mechanisms and practical feasibility. J Environ Sci (China) 93:151–163. https://doi.org/10.1016/j.jes.2020.03.034

Escudey M, Galindo G (1983) Effect of iron oxide coatings on electrophoretic mobility and dispersion of allophane. J Colloid Interface Sci 93:78–83. https://doi.org/10.1016/0021-9797(83)90386-7

Escudey M, Galindo G, Förster JE, Briceño M, Diaz P, Chang A (2001) Chemical Forms of Phosphorus of Volcanic Ash-Derived Soils in Chile. Commun Soil Sci Plant Anal 32:601–616. https://doi.org/10.1081/CSS-100103895

441 Fernández MA, Soulages OE, Acebal SG, Rueda EH, Sánchez RMT (2015) Sorption of Zn(II) and
442 Cu(II) by four Argentinean soils as affected by pH, oxides, organic matter and clay content.
443 Environ Earth Sci 74:4201–4214. https://doi.org/10.1007/s12665-015-4518-0
444 Genrich DA, Bremner JM (1974) Isolation of Soil Particle-Size Fractions. Soil Sci Soc Am J
445 38:222–225. https://doi.org/10.2136/sssaj1974.03615995003800020009x
446 Giese B, Klaessig F, Park B, Kaegi R, Steinfeldt M, Wigger H, Von Gleich A, Gottschalk F (2018)
447 Risks, Release and Concentrations of Engineered Nanomaterial in the Environment. Sci Rep
448 8:1–18. https://doi.org/10.1038/s41598-018-19275-4
449 Hashmi SS, Abbasi BH, Rahman L, Zaka M, Zahir A (2019) Phytosynthesis of organo-metallic
450 silver nanoparticles and their anti-phytopathogenic potency against soil borne *Fusarium spp*.
451 Mater Res Express, 6:1150a9. https://doi.org/10.1088/2053-1591/ab4d7c
452 He J, Wang D, Zhou D (2019) Transport and retention of silver nanoparticles in soil: Effects of
453 input concentration, particle size and surface coating. Sci Total Environ 648:102–108.
454 https://doi.org/10.1016/j.scitotenv.2018.08.136
455 Jiménez JJ, Lal R, Russo RO, Leblanc HA (2008) The soil organic carbon in particle-size separates
456 under different regrowth forest stands of north eastern Costa Rica. Ecol Eng 34:300–310.
457 https://doi.org/10.1016/j.ecoleng.2008.07.001
458 Koopmans GF, Hiemstra T, Vaseur C, Chardon WJ, Voegelin A, Hiemstra T, Vaseur C, Chardon
459 WJ, Voegelin A, Groenenberg JE (2020) Use of iron oxide nanoparticles for immobilizing
460 phosphorus in situ: Increase in soil reactive surface area and effect on soluble phosphorus.
461 Sci Total Environ 711:135220. https://doi.org/10.1016/j.scitotenv.2019.135220
462 Limousin G, Gaudet JP, Charlet L, Szenknect S, Barthès V, Krimissa M (2007) Sorption isotherms:
463 A review on physical bases, modeling and measurement. Appl Geochemistry 22:249–275.
464 https://doi.org/10.1016/j.apgeochem.2006.09.010

Linquist BA, Singleton PW, Yost RS, Cassman KG (1997) Aggregate Size Effects on the Sorption and Release of Phosphorus in an Ultisol. Soil Sci Soc Am J 61:160–166. https://doi.org/10.2136/sssaj1997.03615995006100010024x

Liu G, Xue W, Wang J, Liu X (2019) Transport behavior of variable charge soil particle size fractions and their influence on cadmium transport in saturated porous media. Geoderma 337:945–955. https://doi.org/10.1016/j.geoderma.2018.11.016

Lopez-Lima D, Mtz-Enriquez AI, Carrión G, Basurto-Cereceda S, Pariona N (2021) The bifunctional role of copper nanoparticles in tomato: Effective treatment for *Fusarium* wilt and plant growth promoter. Sci Hortic 277: 109810. https://doi.org/10.1016/j.scienta.2020.109810

Malandrakis AA, Kavroulakis N, Chrysikopoulos CV (2021) Copper nanoparticles against benzimidazole-resistant *Monilinia fructicola* field isolates. Pestic Biochem Physiol 173:104796. https://doi.org/10.1016/j.pestbp.2021.104796

Maslova M V, Ivanenko VI, Yanicheva NY, Mudruk NV (2020) Comparison of The Sorption Kinetics of Lead(II) and Zinc(II) on Titanium Phosphate Ion-Exchanger. Int J Mol Sci 21:447–468. https://doi.org/10.3390/ijms21020447

Molina M, Fuentes R, Calderón R, Escudey M, Avendaño K, Gutiérrez M, Chang AC (2007) Impact of forest fire ash on surface charge characteristics of Andisols. Soil Sci 172:820–834. https://doi.org/10.1097/ss.0b013e31814cee44

Mora ML, Barrow NJ (1996) The effects of time of incubation on the relation between charge and pH of soil. Eur J Soil Sci 47:131–136. https://doi.org/10.1111/j.1365-2389.1996.tb01380.x

Murphy J, Riley JP (1962) A modified single solution method for the determination of phosphate in natural waters. Anal Chim Acta 27:31–36. https://doi.org/10.1057/9781137461131

Parada J, Rubilar O, Diez MC, Cea M, Sant'Ana da Silva A, Rodríguez-Rodríguez CE, Tortella GR (2019) Combined pollution of copper nanoparticles and atrazine in soil: Effects on dissipation of the pesticide and on microbiological community profiles. J Hazard Mater 361:228–236. https://doi.org/10.1016/j.jhazmat.2018.08.042

Parra-Almuna L, Pontigo S, Larama G, Cumming JR, Pérez-Tienda J, Ferrol N, de la Luz Mora M (2020) Expression analysis and functional characterization of two PHT1 family phosphate transporters in ryegrass. Planta 251:1–12. https://doi.org/10.1007/s00425-019-03313-0

Redel Y, Cartes P, Velásquez G, Poblete-Grant P, Poblete-Grant P, Bol R, Mora ML (2016) Assessment of phosphorus status influenced by al and fe compounds in volcanic grassland soils. J Soil Sci Plant Nutr 16:490–506. https://doi.org/10.4067/S0718-95162016005000004

Rolim WR, Lamilla C, Pieretti JC, Díaz M, Tortella GR, Cristina Diez M, Barrientos L, Seabra AB, Rubilar O (2019) Comparison of antibacterial and antibiofilm activities of biologically synthesized silver nanoparticles against several bacterial strains of medical interest. Energy, Ecol Environ 4:143–159. https://doi.org/10.1007/s40974-019-00123-8

Sadzawka RA, Carrasco RMA, Grez ZR, Mora GM de la L, Flores PH, Neaman A (2006) Métodos de análisis recomendados para suelos chilenos. Comisión de Normalización y Acreditación (CNA). Sociedad Chilena de la Ciencia del Suelo

Soliemanzadeh A, Fekri M, Bakhtiary S, Hejazi M (2016) Biosynthesis of iron nanoparticles and their application in removing phosphorus from aqueous solutions. Chem Ecol 32:286–300. https://doi.org/10.1080/02757540.2016.1139091

Song Z, Liu H, Zhao F, Xu C (2014) Ecological stoichiometry of N:P:Si in China's grasslands. Plant Soil 380:165–179. https://doi.org/10.1007/s11104-014-2084-y

Sparks DL (2003) Environmental soil chemistry: an overview. In: Sparks DL (ed) Environmental Soil Chemistry, 2nd edn. Academic Press, London, pp. 1-42

512 Spohn M (2020) Phosphorus and carbon in soil particle size fractions: A synthesis.
513 Biogeochemistry 147:225–242. https://doi.org/10.1007/s10533-019-00633-x
514 Suazo-Hernández J, Klumpp E, Arancibia-Miranda N, Poblete-Grant P, Jara A, Bol R, Mora
515 MDLL (2021) Describing Phosphorus Sorption Processes on Volcanic Soil in the Presence
516 of Copper or Silver Engineered Nanoparticles. Minerals 11:1–18.
517 https://doi.org/10.3390/min11040373
518 Sun T, Deng L, Fei K, Zhang L, Fan X (2020) Characteristics of phosphorus adsorption and
519 desorption in erosive weathered granite area and effects of soil properties. Environ Sci
520 Pollut Res 28780–28793. https://doi.org/10.1007/s11356-020-08867-1
521 Taghipour M, Jalali M (2015) Effect of nanoparticles on kinetics release and fractionation of
522 phosphorus. J Hazard Mater 283:359–370. https://doi.org/10.1016/j.jhazmat.2014.09.045
523 Van Nguyen D, Nguyen HM, Le NT, Nguyen KH, Nguyen HT, Le HM, Nguyen AT, Dinh NTT,
524 Hoang SA, Van Ha C (2021) Copper Nanoparticle Application Enhances Plant Growth and
525 Grain Yield in Maize Under Drought Stress Conditions. J Plant Growth Regul 41:364–375.
526 https://doi.org/10.1007/s00344-021-10301-w
527 Yang X, Chen X, Yang X (2019) Effect of organic matter on phosphorus adsorption and desorption
528 in a black soil from Northeast China. Soil Tillage Res 187:85–91.
529 https://doi.org/10.1016/j.still.2018.11.016
530 Yin Q, Ren H, Wang R, Zhao Z (2018) Evaluation of nitrate and phosphate adsorption on Al-
531 modified biochar: Influence of Al content. Sci Total Environ 631–632:895–903.
532 https://doi.org/10.1016/j.scitotenv.2018.03.091
533 Zhao Z, Jin R, Fang D, Wang H, Dong Y, Xu R, Jiang J (2018) Paddy cultivation significantly
534 alters the forms and contents of Fe oxides in an Oxisol and increases phosphate mobility. Soil
535 Tillage Res 184:176–180. https://doi.org/10.1016/j.still.2018.07.012

536 Zhou A, Tang H, Wang D (2005) Phosphorus adsorption on natural sediments: Modeling and
537 effects of pH and sediment composition. Water Res 39:1245–1254.
538 https://doi.org/10.1016/j.watres.2005.01.026
539
540
541

Tables

Table 1 Physicochemical properties and stoichiometry molar ratios of C, N, and P of soil particle size fractions.

Parameter	2000-32 µm	32-2 µm	<2 µm
Mass (%)	16.2	59.3	24.5
pH (H_2O)	5.6 ± 0.1	6.0 ± 0.0	6.2 ± 0.1
Total C (g kg^{-1})	65.0 ± 0.43	70.8 ± 0.4	101.2 ± 0.2
Total N (g kg^{-1})	5.2 ± 0.2	6.1 ± 0.0	11.3 ± 0.1
Total P (g kg^{-1})	1.2 ± 0.0	1.4 ± 0.3	2.4 ± 0.1
C:N molar ratio	14.5	13.6	10.5
C:P molar ratio	145.1	129.7	107.9
N:P molar ratio	10.0	9.6	10.3
C:N:P molar ratio	145:10:1	119:8:1	69:5:1
K ($cmol_{(+)}$ kg^{-1})	0.7 ± 0.1	0.6 ± 0.0	0.9 ± 0.1
Na ($cmol_{(+)}$ kg^{-1})	0.3 ± 0.0	0.7 ± 0.1	0.1 ± 0.0
Ca ($cmol_{(+)}$ kg^{-1})	5.4 ± 0.2	3.8 ± 0.2	6.7 ± 0.2
Mg ($cmol_{(+)}$ kg^{-1})	1.0 ± 0.0	1.6 ± 0.2	1.4 ± 0.2
Al ($cmol_{(+)}$ kg^{-1})	0.1 ± 0.0	0.1 ± 0.0	0.5 ± 0.0
ECEC ($cmol_{(+)}$ kg^{-1})[a]	7.5 ± 0.1	6.7 ± 0.1	9.6 ± 0.1
Specific surface area (m^2 g^{-1})	7.34	10.85	22.76

[a]ECEC: Effective cation exchange capacity.

Table 2 Elovich parameters (± standard error) of soil particle size fractions obtained from phosphate adsorption kinetics in the presence and absence of Ag or Cu ENPs at pH 5.5 ± 0.2.

		Elovich model				
Soil particle size fractions	**ENPs (%)**	**α** **(x 10^2 mmol kg^{-1} min^{-1})**	**β** **(x 10^{-2} mmol kg^{-1})**	**log K_{eq}**	**r^2**	**χ^2**
2000-32 µm	**0**	13.73 ± 1.13	8.29 ± 0.38	4.21	0.960	62
32-2 µm		20.34 ± 2.98	8.00 ± 0.06	4.40	0.976	39
<2 µm		6.71 ± 0.98	5.94 ± 0.40	4.05	0.981	49
			Ag			
2000-32 µm		20.18 ± 1.73	7.06 ± 0.31	4.46	0.987	27
32-2 µm	**3**	6.55 ± 0.69	5.17 ± 0.21	4.10	0.979	58
<2 µm		24.33 ± 1.83	5.30 ± 0.20	4.66	0.967	127
2000-32 µm		13.08 ± 0.09	6.24 ± 0.23	4.32	0.992	21
32-2 µm	**5**	8.49 ± 0.50	5.61 ± 0.11	4.18	0.986	40
<2 µm		39.98 ± 1.14	5.04 ± 0.12	4.90	0.985	65
			Cu			
2000-32 µm		53.25 ± 7.19	7.45 ± 0.44	4.85	0.989	25
32-2 µm	**3**	317.40 ± 30.44	7.81 ± 0.78	5.61	0.975	65
<2 µm		34.42 ± 2.82	5.36 ± 0.61	4.81	0.956	182
2000-32 µm		32.14 ± 3.72	6.26 ± 0.40	4.71	0.986	42
32-2 µm	**5**	124.46 ± 14.24	6.50 ± 0.39	5.28	0.989	34
<2 µm		26.62 ± 4.52	4.66 ± 0.25	4.76	0.989	53

Table 3 Langmuir-Freundlich parameters (± standard error) of soil particle size fractions obtained from phosphate adsorption isotherms in the presence and absence of Ag or Cu ENPs at pH 5.5 ± 0.2.

Langmuir-Freundlich model						
Soil particle size fractions	**ENPs (%)**	**q_{max} (mmol kg^{-1})**	**K_{L-F} (L kg^{-1})**	**n**	**r^2**	**χ^2**
2000-32 µm	**0**	180.01 ± 17.17	1.73 ± 0.46	1.77 ± 0.16	0.988	39
32-2 µm		211.15 ± 14.33	1.64 ± 0.20	1.69 ± 0.10	0.988	47
<2 µm		264.58 ± 25.36	1.82 ± 0.28	2.02 ± 0.14	0.958	239
			Ag			
2000-32 µm	**3**	202.20 ± 24.50	2.99 ± 0.54	1.31 ± 0.26	0.963	182
32-2 µm		232.10 ± 11.50	7.77 ± 1.48	1.07 ± 0.14	0.984	112
<2 µm		279.39 ± 18.36	4.34 ± 0.47	1.35± 0.20	0.990	85
2000-32 µm	**5**	227.20 ± 16.11	4.25 ± 0.58	1.05 ± 0.17	0.973	181
32-2 µm		245.41 ±12.32	10.76 ± 1.92	0.85 ± 0.13	0.978	184
<2 µm		344.44 ± 17.42	2.34 ± 0.32	1.51 ± 0.14	0.995	51
			Cu			
2000-32 µm	**3**	207.07 ± 7.02	9.31 ± 1.16	0.78 ± 0.09	0.990	60
32-2 µm		230.84 ± 9.54	16.36 ± 2.14	0.64 ± 0.03	0.983	134
<2 µm		287.00 ± 15.88	4.82 ± 2.42	1.09 ± 0.18	0.978	200
2000-32 µm	**5**	245.54 ± 19.02	5.80 ± 0.70	0.89 ± 0.13	0.943	419
32-2 µm		277.81 ± 15.84	14.43 ± 1.26	0.69 ± 0.08	0.981	191
<2 µm		339.93 ± 10.30	3.97 ± 0.85	0.94 ± 0.13	0.986	154

Table 4 Phosphate desorption (%) (± standard error) obtained from soil particle size fractions in the presence and absence of Ag or Cu ENPs after shaking with double-distilled water for 24 h at 20 ± 2 ºC.

Phosphate desorbed (%)					
Soil particle size fractions	**ENPs (%)**	**Desorption cycle**			**Total desorbed**
		1	**2**	**3**	
2000-32 µm	**0**	13.70 ± 1.51	9.66 ± 0.42	7.39 ± 0.02	30.76 ± 1.22
32-2 µm		15.36 ± 2.23	12.00 ± 0.83	7.55 ± 0.63	34.92 ± 1.48
<2 µm		11.88 ± 1.99	7.37 ± 0.24	5.00 ± 0.03	24.25 ± 1.02
				Ag	
2000-32 µm	**3**	11.79 ± 1.33	7.89 ± 0.05	6.26 ± 0.08	25.94 ± 1.64
32-2 µm		7.60 ± 0.62	6.35 ± 0.08	5.06 ± 0.06	19.01 ± 0.69
<2 µm		11.42 ± 1.60	7.67 ± 0.29	4.57 ± 0.19	23.66 ± 0.98
2000-32 µm	**5**	9.94 ± 1.53	7.39 ± 0.23	5.68 ± 0.31	23.01 ± 1.07
32-2 µm		6.40 ± 0.94	5.10 ± 0.26	4.25 ± 0.21	15.75 ± 0.58
<2 µm		9.20 ± 1.01	6.34 ± 0.07	3.85 ± 0.05	19.40 ± 0.55
				Cu	
2000-32 µm	**3**	8.81 ± 1.93	9.15 ± 0.24	6.02 ± 0.34	23.98 ± 0.99
32-2 µm		6.33 ± 0.35	5.42 ± 0.38	4.53 ± 0.28	16.28 ± 0.68
<2 µm		7.86 ± 1.70	5.46 ± 0.16	3.68 ± 0.07	17.00 ± 1.25
2000-32 µm	**5**	7.47 ± 1.41	6.67 ± 0.63	4.53 ± 0.15	18.67 ± 0.80
32-2 µm		4.94 ± 0.41	4.25 ± 0.21	2.42 ± 0.02	11.61 ± 0.24
<2 µm		5.41 ± 0.77	4.79 ± 0.35	2.63 ± 0.21	12.84 ± 0.83

Figure captions

Fig. 1 Zeta potential (ZP) measurement of different soil particle size fractions at various pH values in 0.01 mol L^{-1} KCl.

Fig. 2 Kinetics of phosphate (Pi) adsorption at pH 5.5 ± 0.2 in the presence and absence of Ag ENPs on (a) 2000-32 μm, (b) 32-2 μm, and (c) <2 μm fractions or Cu ENPs on (d) 2000-32 μm, (e) 32-2 μm, and (f) <2 μm fractions, fitted using the Elovich model.

Fig. 3 Isotherms of phosphate (Pi) adsorption at pH 5.5 ± 0.2 in the presence and absence of Ag ENPs on (a) 2000-32 μm, (b) 32-2 μm, and (c) <2 μm fractions or Cu ENPs on (d) 2000-32 μm, (e) 32-2 μm, and (f) <2 μm fractions, fitted using the Langmuir-Freundlich model.

Fig. 4 The pH-zeta potential curves (ZP) post-adsorption 9.71 mmol L^{-1} phosphate (Pi) in the presence and absence of 5% Ag or Cu ENPs at constant ionic strength (0.01 mol L^{-1} KCl) (a) 2000-32 μm, (b) 32-2 μm, and (c) <2 μm fractions.

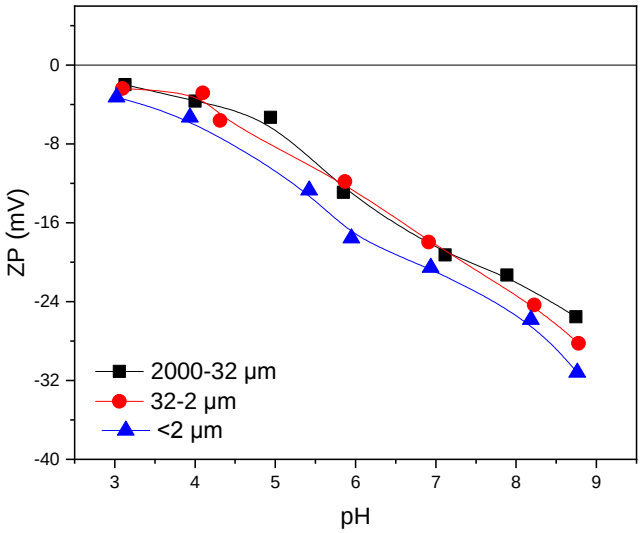

Fig. 1

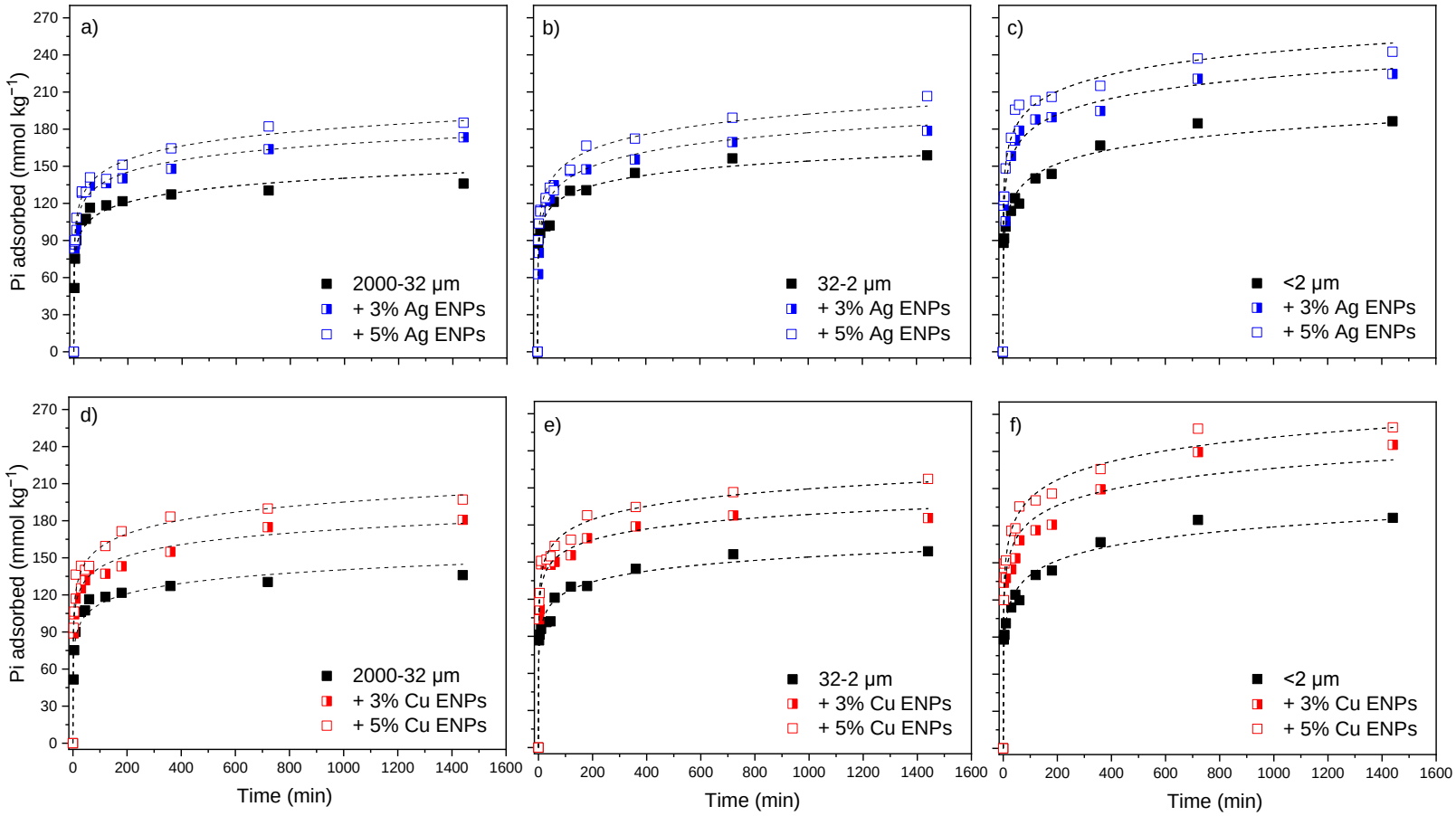
a)
b)
c)
d)
e)
f)
Pi adsorbed (mmol kg^{-1})
Time (min)
2000-32 µm
+ 3% Ag ENPs
+ 5% Ag ENPs
32-2 µm
+ 3% Ag ENPs
+ 5% Ag ENPs
<2 µm
+ 3% Ag ENPs
+ 5% Ag ENPs
2000-32 µm
+ 3% Cu ENPs
+ 5% Cu ENPs
32-2 µm
+ 3% Cu ENPs
+ 5% Cu ENPs
<2 µm
+ 3% Cu ENPs
+ 5% Cu ENPs

Fig. 2

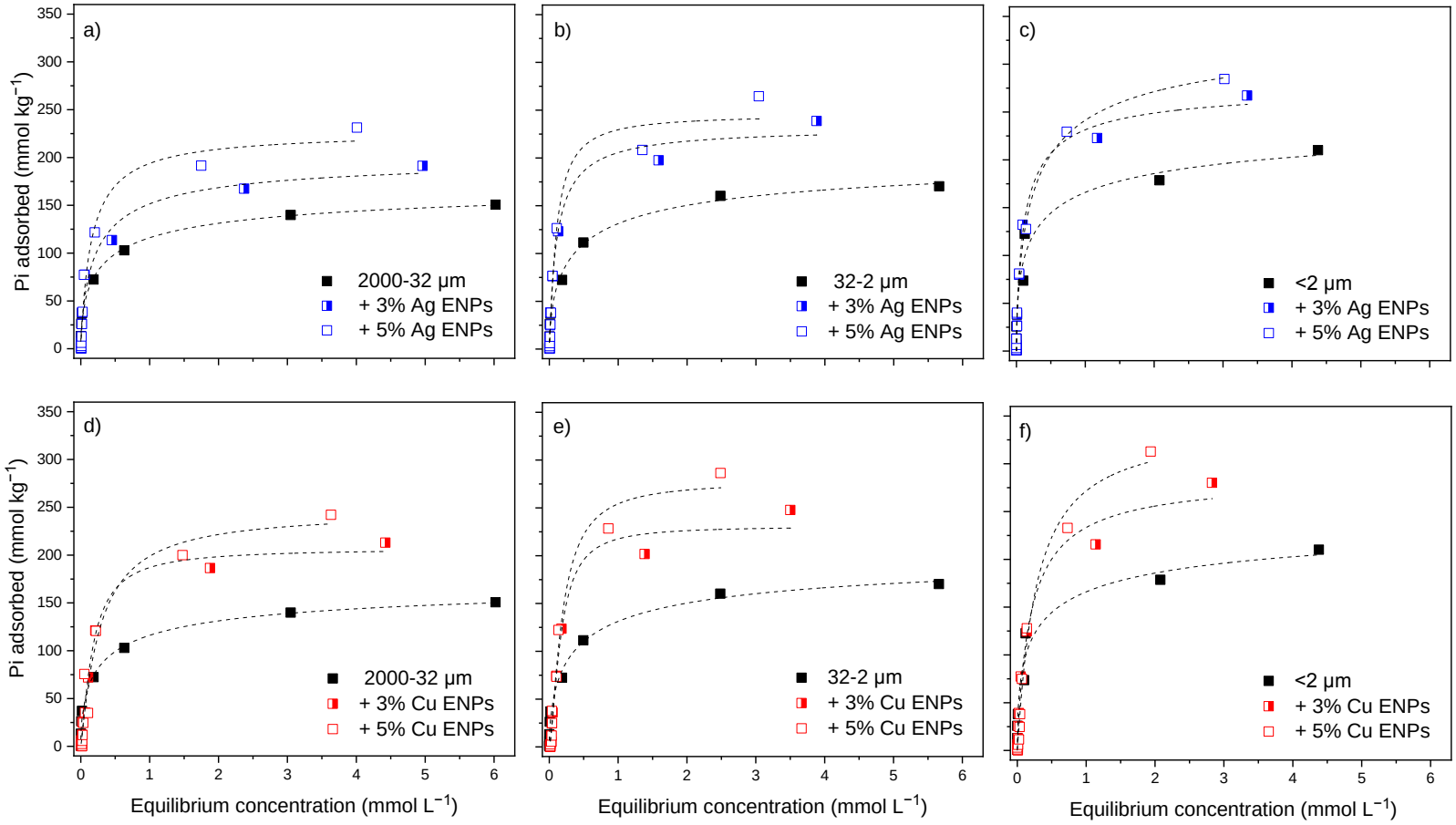
a)
b)
c)
d)
e)
f)
Pi adsorbed (mmol kg^{-1})
Equilibrium concentration (mmol L^{-1})
2000-32 µm
32-2 µm
<2 µm
+ 3% Ag ENPs
+ 5% Ag ENPs
+ 3% Cu ENPs
+ 5% Cu ENPs

Fig. 3

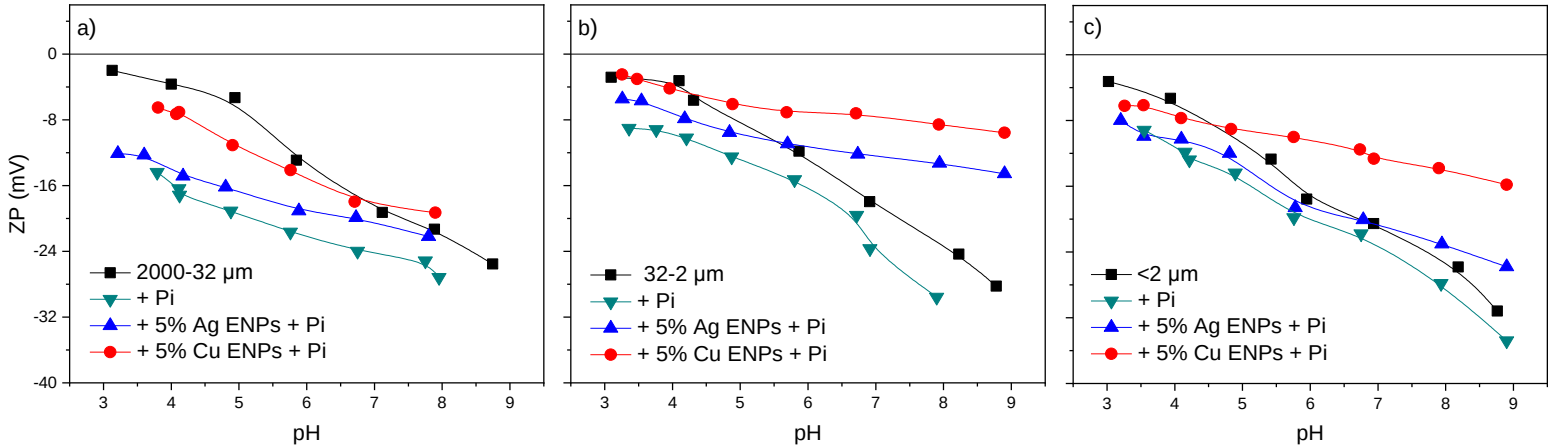
a)
b)
c)
ZP (mV)
0
-8
-16
-24
-32
-40
3
4
5
6
7
8
9
pH
2000-32 µm
+ Pi
+ 5% Ag ENPs + Pi
+ 5% Cu ENPs + Pi
32-2 µm
<2 µm

Fig. 4